

# Physical and Numerical Studies of a Fracture System Model

ANDREW R. PIGGOTT AND DEREK ELSWORTH<sup>1</sup>

*Department of Mineral Engineering, The Pennsylvania State University, University Park*

Physical and numerical studies of transient flow in a model of discretely fractured rock are presented. The physical model is a thermal analogue to fractured media flow consisting of idealized disc-shaped fractures. The numerical model is used to predict the behavior of the physical model. The use of different insulating materials to encase the physical model allows the effects of differing leakage magnitudes to be examined. A procedure for determining appropriate leakage parameters is documented. These parameters are used in forward analysis to predict the thermal response of the physical model. Knowledge of the leakage parameters and of the temporal variation of boundary conditions are shown to be essential to an accurate prediction. Favorable agreement is illustrated between numerical and physical results. The physical model provides a data source for the benchmarking of alternative numerical algorithms.

## INTRODUCTION

The recent accelerated development of codes describing flow in three-dimensional discretely fractured media (see, for example, *Huang and Evans [1985]*, *Long et al. [1985]*, *Piggott [1986]*, and *Andersson and Dverstorp [1987]*) has occurred with only a limited opportunity for evaluating the performance of the algorithms. The codes are, by their nature, developed to describe extremely heterogeneous conditions. These conditions preclude the derivation of analytical results. Although the individual components of a discrete fracture model may be rigorously validated against alternative numerical schemes [*Elsworth, 1986a, b*], questions remain as to the performance of the assembled system.

A numerical approach to discrete fracture hydraulics is justifiable only when it can be demonstrated that the inherent idealization is geologically plausible and that the algorithm accurately simulates the behavior of the idealized system. The first issue is currently open to debate; the second issue forms the basis of this paper.

Problems entrained in the hydraulic analysis of intersecting disc systems relate both to the ability of a numerical formulation to accommodate the governing equations and to the adequacy of the spatial and temporal discretization of the system. The degree of approximation that results is inversely proportional to the density of nodal coverage. Computational economy demands that the degree of discretization be minimized if complex fracture systems are to be investigated. Clearly, an accurate yet economical numerical algorithm is necessary.

In the absence of closed-form solutions for flow in nontrivial fracture systems, it is necessary to identify alternate means of validation. One approach which could be adopted involves the comparison of numerically predicted responses with those collected from field tests conducted in a fracture dominated aquifer. This approach is desirable, since it directly addresses the physical problem considered by fracture hydraulics research. Such a study, while ultimately necessary, complicates validation by superimposing the uncertainty of the geological

environment on the physics of the problem. An alternate approach is based on the use of a physical model to generate responses which may then be compared to those predicted by the numerical formulation. Models used to study groundwater hydraulics are based on the similarity of the governing equations for hydraulic, electrical, and thermal flow. The use of physical models in both the validation of analytical solutions and the investigation of physical phenomena is not without precedent. Previous researchers have documented the use of electrical [*Sharp, 1970*; *Hudson and LaPointe, 1980*; *Tsang, 1984*], thermal [*Javandel and Witherspoon, 1967*], and hydraulic models [*Wilson, 1970*; *Hull et al., 1987*]. The difficulties associated with the fabrication and operation of hydraulic and electrical models render thermal modeling the most suitable alternative for simulating transient fluid flow in discrete rock fractures. Table 1 summarizes the analogies existing between hydraulic and thermal flow. The following describes an attempt to predict the transient response of a thermal analogue fracture system model using a documented numerical procedure.

## PHYSICAL MODEL

The physical model consists of 12 planar discs which correspond to the discrete members of an orthogonal fracture system with each of the three mutually orthogonal orientations represented by four discs. The disc system is, by definition, truncated by the boundaries of a cubic volume. The discs are circular in shape but are frequently truncated as required by the boundaries of the cube. The system was automatically generated, geometrically analyzed, and reduced to a form suitable for fabrication and numerical analysis according to the procedure described by *Piggott [1986]*. The discs are 2 mm thick 70-30 brass and have a diameter of 0.3 m. The cube also has a dimension of 0.3 m. Soldered connections join the discs along their intersection segments. The high thermal conductivity and low thermal mass of the soldered connections represent a near-perfect thermal connection between joined discs. A brass baseplate was added in order to improve the structural integrity of the model. The completed model is illustrated schematically in Figure 1. Insulation is located between the discs and surrounding the model. The thermal properties of the model are summarized in Table 2. A thermal disturbance is applied to the model by contacting the baseplate with an ice bath. All other cube surfaces act as impermeable boundaries.

The temperature monitoring system used in conjunction

<sup>1</sup>Now at Waterloo Centre for Groundwater Research, University of Waterloo, Waterloo, Ontario, Canada.

TABLE 1. Hydraulic and Thermal Analogies

Hydraulic Analogy	Thermal Analogy
Hydraulic head	temperature
Darcy's law	Fourier's law
Hydraulic conductivity	thermal conductivity
Specific storage	specific heat times mass density
Hydraulic diffusivity	thermal diffusivity
Leakage coefficient	heat transfer coefficient

with the model consists of an Omega model 2166A-J multi-point digital thermometer and Omega style III, type J iron-constantan thermocouples. The monitoring system has an accuracy of 1°C in the range of temperatures considered and responds sufficiently rapidly to capture the transient response of the model. The thermocouples are located along disc intersections at positions coincident with those of identifiable nodes in the numerical model. The locations of thermocouples relative to the baseplate are given in Table 3. Thermal paths joining the baseplate and two points at the same distance from the baseplate are unique, and therefore thermocouple positioning is of little significance in the absence of detailed model geometry. Data concerning the exact positioning and interconnection of discs together with absolute locations of thermocouples are recorded in the work by Piggott and Elsworth [1987]. Figure 2 shows details of the positioning of the thermocouples which are assumed to measure boundary condition temperatures, that is, the temperature applied to the disc system by the baseplate. The boundary condition thermocouples are separated from the constant temperature of the ice bath by the wall of the ice bath, the baseplate, and most likely an air gap. The temperatures measured by these thermocouples are transient and are related to the temperature of the ice bath by the thermal properties of the disc model and of the materials separating them from the ice bath. Three tests have been conducted on the model to date. During test 1, the model was instrumented with thermocouples designated A-1 through A-8 and insulated with styrofoam packing material. The model was then reinstrumented for tests 2 and 3 with thermocouples designated B-1 through B-9 and insulated with foamed-in-place polyurethane further surrounded by fiberglass insulation. The positions of A and B series thermocouples are not related. Test 3 corresponds to the recovery phase of test 2 wherein the ice bath was removed and the model allowed to recover to room temperature.

The data obtained during the tests was transformed into reduced quantities. Temperature is expressed in normalized form using

$$T_n = (T - T_0)/(T_{bc} - T_0) \quad (1)$$

where  $T_n$  is the normalized temperature corresponding to temperature  $T$ , initial temperature  $T_0$ , and steady state boundary condition temperature  $T_{bc}$ . Normalized temperatures of zero and unity correspond to initial and steady state boundary condition temperatures, respectively. Time is expressed in dimensionless form using

$$t_d = Dt/d^2 \quad (2)$$

where  $t_d$  is the dimensionless time corresponding to thermal diffusivity  $D$ , time  $t$ , and disc diameter  $d$ . The potential for

heat transfer from the insulation to the discs is expressed in dimensionless form using

$$d_a = d(k'/Kb)^{1/2} \quad (3)$$

where  $d_a$  is the dimensionless disc diameter corresponding to a disc diameter of  $d$ , heat transfer coefficient  $k'$ , thermal conductivity  $K$ , and disc thickness  $b$ . A dimensionless diameter of zero signifies perfectly insulated (confined) behavior. Dimensionless diameter is analogous to dimensionless radius as defined in semiconfined aquifer theory (see, for example, Kruseman and DeRidder [1983]) where the hydraulic counterpart of the heat transfer coefficient is the leakage coefficient of Hantush and Jacob [1955]. Moench [1984] suggests that semiconfined behavior is applicable to the description of dual-porosity flow where the head contrast between fracture and matrix is restricted to the vicinity of the fracture matrix contact and that such conditions are characteristic of low conductivity contacts.

#### NUMERICAL MODEL

The numerical model of the fracture system is based upon the application of the hybrid boundary element-finite element approach described by Elsworth [1986a] and automated by Piggott [1986]. The baseplate of the physical model has no counterpart in the numerical model. Figure 3 shows the discretized representation of a typical fracture disc. The boundary element formulation requires only that the disc perimeter and intersection slits be represented. Those nodes defining the impermeable portion of the disc perimeter (local nodes) have degrees of freedom which are condensed out of the conductance matrix at the level of a single disc. Nodes defining intersection slits and permeable portions of the disc perimeter (global nodes) are retained for the assembly of the conductance matrix governing the fracture system. The geometry of the disc system is described by a total of 242 nodes of which 61 are global nodes. Among the global nodes, 45 possess active degrees of freedom and 16 are located along the specified head boundary condition surface represented by the baseplate in the physical model. The boundary element formulation applied to the model is especially suitable for linear flow within fractures of high area to perimeter ratios and possessing homogeneous and isotropic properties. Further details of the formulation are given by Elsworth [1986a] to which the interested reader is referred.

The boundary element formulation ultimately yields a system of equations of the form

$$q_c = Kh \quad (4)$$

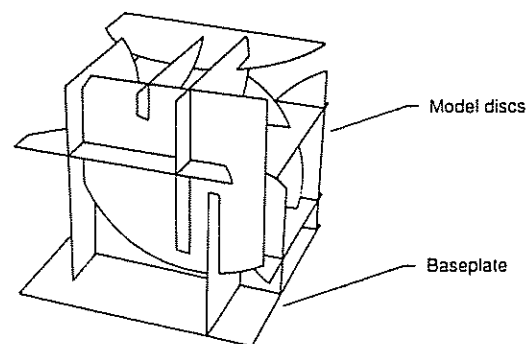


Fig. 1. Schematic illustration of the fracture system model.

TABLE 2. Thermal Diffusivities of Model Materials

Material	Thermal Diffusivity, m <sup>2</sup> /s	Reference
70-30 brass	3.75 × 10 <sup>-5</sup>	American Society of Metals [1979]
Polyurethane foam	1.8 × 10 <sup>-10</sup>	Turner and Malloy [1981]
Fiberglass	7.2 × 10 <sup>-10</sup>	Turner and Malloy [1981]
Air (20°C)	2.1 × 10 <sup>-5</sup>	Eckert and Drake [1959]

for each fracture where  $q_c$  is a vector of nodal discharges due to conduction in the fracture,  $K$  is the conductance matrix defined by the geometry and transmissivity of the fracture, and  $h$  is a vector of nodal heads.

The rate at which fluid enters a fracture from the matrix due to leakage is given by

$$v_l = -k'(h - h_r) \tag{5}$$

where  $v_l$  is the leakage velocity,  $k'$  is the leakage coefficient,  $h$  is the head in the fracture, and  $h_r$  is the reference head in the matrix. The total volume of fluid entering a fracture per unit time due to leakage is given by

$$q_l = -k' \int_A (h - h_r) dA \tag{6}$$

where  $A$  is the plan area of the fracture. Equation (6) may be restated in finite element form as

$$q_l = -k'AW(h - h_r) \tag{7}$$

which reduces to

$$q_l = L(h - h_r) \tag{8}$$

where  $q_l$  is a vector of nodal discharges due to leakage,  $W$  is the nodal weighting matrix,  $h$  is a vector of nodal heads,  $h_r$  is the vector of nodal reference heads, and  $L$  is the lumped leakage matrix for the domain. The individual terms for the nodal weighting matrix ( $W$ ) are given by

$$W_{ij} = \delta_{ij}K_{ij}/K_{kk} \tag{9}$$

where  $\delta_{ij}$  is the Kronecker delta,  $K_{ij}$  are the terms of the conductance matrix, and  $K_{kk}$  is the trace of the conductance matrix. The conductance matrix written for an individual disc is fully populated. During transient behavior, the rate at which fluid is released from storage within the fracture is given by

$$v_s = -S_s b \dot{h} \tag{10}$$

where  $v_s$  is the storage depletion velocity,  $S_s$  is the specific storage,  $b$  is the fracture aperture, and  $\dot{h}$  is the time derivative of head. The total quantity of fluid entering a fracture from storage within the fracture per unit time is given by

$$q_s = -S_s b \int_A \dot{h} dA \tag{11}$$

Equation (11) may be restated in finite element form as

$$q_s = S_s b A W \dot{h} \tag{12}$$

which reduces to

$$q_s = S \dot{h} \tag{13}$$

where  $q_s$  is a vector of nodal discharges due to storage depletion,  $\dot{h}$  is a vector of nodal time derivatives of head, and  $S$  is the lumped storativity matrix for the fracture.

The summation of the conductance, leakage, and storativity matrices for all fracture domains yields matrices representing the fracture system. Applying continuity to (4), (8), and (13) leads to

$$Kh + L(h - h_r) + S\dot{h} = q \tag{14}$$

where  $q$  is a vector of nodal discharges. The vector of time derivatives of head  $\dot{h}$  may be approximated using the backward difference formula

$$\dot{h}_{t+\Delta t} = 1/\Delta t (h_{t+\Delta t} - h_t) \tag{15}$$

where  $h_t$  and  $h_{t+\Delta t}$  are vectors of nodal head at times  $t$  and  $t + \Delta t$ . Expressed in compact form, (14) becomes

$$K^* h_{t+\Delta t} = q_{t+\Delta t}^* \tag{16}$$

where

$$K^* = K + L + 1/\Delta t S \tag{17}$$

$$q_{t+\Delta t}^* = q_{t+\Delta t} + Lh_r + 1/\Delta t Sh_t \tag{18}$$

TABLE 3. Thermocouple Locations

Thermocouple	Distance From Baseplate, m
A-1 and A-2	0*
A-3 and A-4 (duplicates)	0.175
A-5	0.169
A-6	0.160
A-7 and A-8	0.270
B-1 and B-2	0.270
B-3	0.132
B-4	0.169
B-5	0.175
B-6	0.212
B-7	0*
B-8	0.189
B-9	0.279

\*Thermocouples measuring boundary condition temperatures.

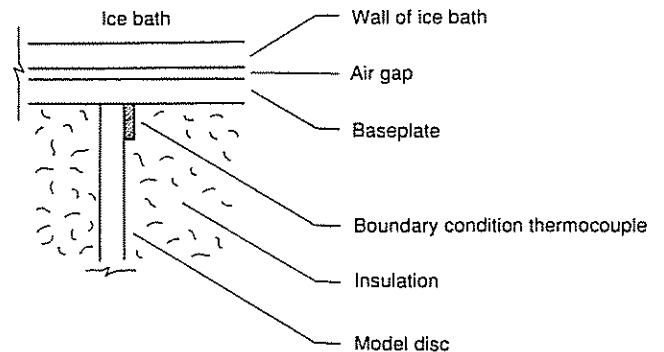


Fig. 2. Schematic cross section of the fracture system model showing the application of boundary conditions and the location of boundary condition thermocouples.

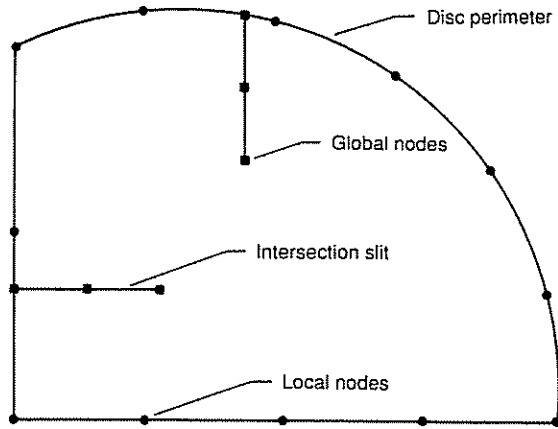


Fig. 3. Discretized representation of a typical disc.

Time-dependent boundary conditions are applied to the numerical model by specifying nodal values of  $h_{i+\Delta t}$  in (16) and of  $q_{i+\Delta t}$  in (18) which correspond to time  $t + \Delta t$ . Transient behavior is evaluated by direct integration of (16).

The response of the numerical model may be expressed in the same manner as the response of the physical model; that is, normalized temperature versus dimensionless time. Again, hydraulic head is analogous to temperature and is used in lieu of temperature in (1).

In addition to the following comparison to a physical model, the numerical formulation has been extensively validated against analytical solutions for both steady state and transient flow in confined and semiconfined axisymmetric systems.

INTERPRETATION AND PREDICTION OF MODEL BEHAVIOR

*Elsworth and Piggott [1987]* describe an attempt to apply a nonleaky form of the numerical model to the prediction of the response of the physical model during test 1. Predictive errors were observed at small and large dimensionless times while acceptable predictions were obtained for intermediate dimensionless times. The failure of the numerical model at large dimensionless times is attributed to heat transfer between the insulation and disc system. Thermal leakage is not sufficient to explain the poor agreement observed at small dimensionless times. The numerical model applied by *Elsworth and Piggott* assumes a constant normalized boundary condition temper-

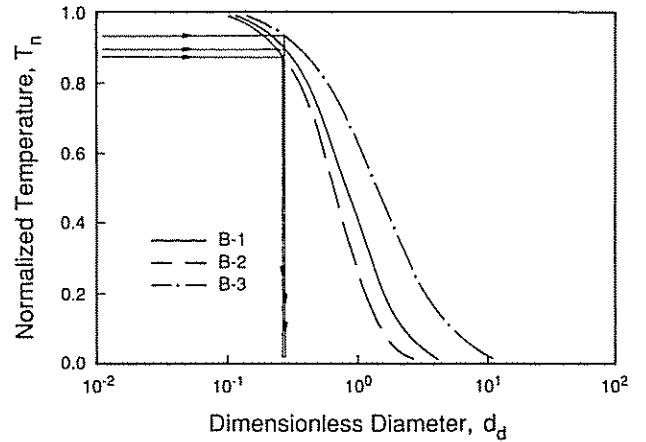


Fig. 5. Variation of steady state normalized temperature with dimensionless diameter for selected B series thermocouples.

ature of unity applied to the model at a dimensionless time of zero. As discussed previously, the actual boundary conditions are transient. The inconsistency in the applied boundary conditions is suggested as the cause of the predictive error at small dimensionless times.

Figures 4 and 5 show the variation of steady state normalized temperatures with dimensionless diameter for selected A and B series thermocouples. These curves were prepared by substituting a range of values of the leakage coefficient into (7) and obtaining a steady state solution to (16). Apparent steady state normalized temperatures of 0.82, 0.64, and 0.70 were observed for thermocouples A-6 through A-8 for test 1. Entering Figure 4 with these values suggests a dimensionless diameter of approximately 0.51. Repeating the process for the remaining A series thermocouples yields an average dimensionless diameter of 0.53 which is taken to be characteristic of the insulating properties of the styrofoam packing material. Apparent steady state normalized temperatures of 0.89, 0.87, and 0.93 were observed for thermocouples B-1 through B-3 for test 2. Entering Figure 5 with these values and averaging the resulting dimensionless diameters with those obtained from the remaining thermocouples yields a dimensionless diameter of 0.28. This value is taken to be characteristic of the polyurethane foam used as insulation during tests 2 and 3. This procedure for estimating the dimensionless diameter cannot be applied to the results of test 3 as the thermocouples, by the

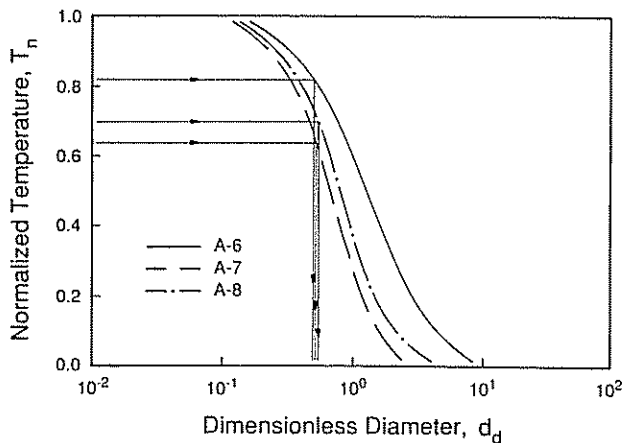


Fig. 4. Variation of steady state normalized temperature with dimensionless diameter for selected A series thermocouples.

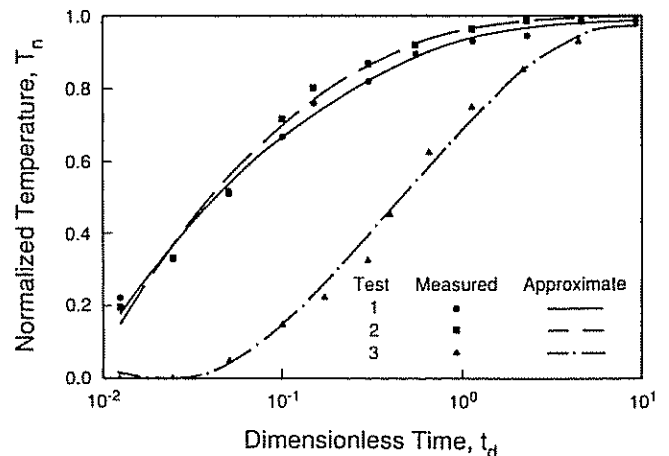


Fig. 6. Variation of normalized boundary condition temperatures with dimensionless time.

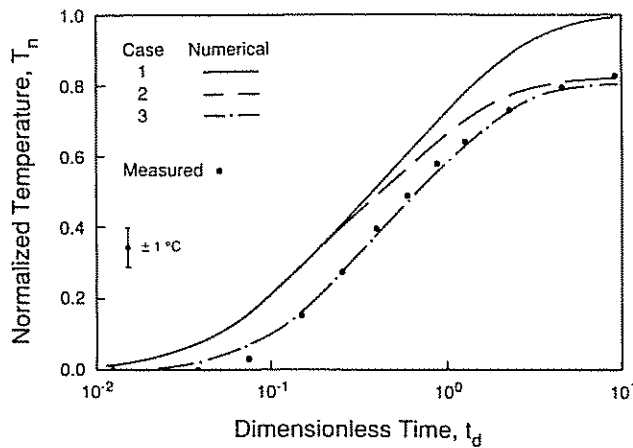


Fig. 7. Measured and various predicted thermal responses of thermocouple A-6 for test 1.

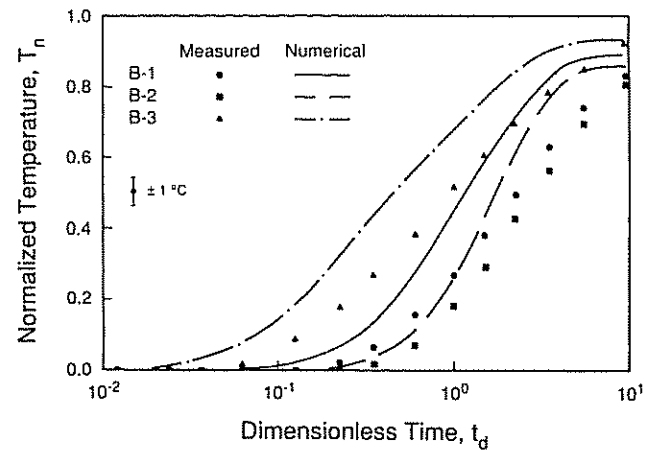


Fig. 9. Measured and predicted thermal responses for test 2.

nature of the test, reach a steady state normalized temperature of unity. Once the dimensionless diameter has been estimated, the appropriate leakage coefficient may be determined by substituting the known values of dimensionless diameter, disc diameter, conductivity, and disc thickness into (3).

Figure 6 shows the variation of the measured normalized boundary condition temperatures with dimensionless time for tests 1 through 3. The measured data in Figure 6 are approximated by third-order polynomial functions fit to the data using the least squares procedure described by Atkinson [1978]. By incorporating the approximating polynomials into the computational algorithm, it is possible to represent the transient nature of the boundary conditions without the need to quantify the thermal properties of the materials separating the model discs from the ice bath.

Figure 7 shows the measured response of thermocouple A-6 during test 1 as well as the numerically predicted response for three modeling scenarios. Case 1 corresponds to a constant normalized boundary condition temperature of unity applied at time zero and to the assumption of perfectly insulated (confined) behavior. Case 1 is typical of the results presented by Elsworth and Piggott [1987]. Case 2 corresponds to constant boundary conditions and a dimensionless diameter of 0.53. Case 3 corresponds to transient boundary conditions and a dimensionless diameter of 0.53. The best agreement between measured and predicted responses is obtained for case 3 and,

for this reason, transient boundary conditions and semi-confined behavior will be assumed in the remaining analysis. All predicted responses presented in this paper were obtained from numerical integration based on 40 dimensionless time increments of 0.01 followed by 60 increments of 0.06 and then by 30 increments of 0.20.

Figures 8 through 10 show measured and predicted responses for tests 1 through 3, respectively. Thermocouples A-6 through A-8 and B-1 through B-3 were selected in order to illustrate rapid, intermediate, and slow thermal responses. The agreement between measured and predicted responses for the remaining thermocouples is of equal quality. Excellent agreement between the measured and predicted responses is apparent for tests 1 and 3. The numerical model consistently overestimates the response of the physical model for test 2. It is suggested that the relatively poor agreement between the measured and predicted responses for test 2 are due to experimental inadequacies. A nonuniform temperature distribution on the baseplate is suspected.

CONCLUSIONS

The physical model represents a thermal analogue to a system of hydraulically conductive discrete rock fractures. The tests conducted on the model provide transient data which may be used to evaluate the performance of computational approaches to fracture hydraulics.

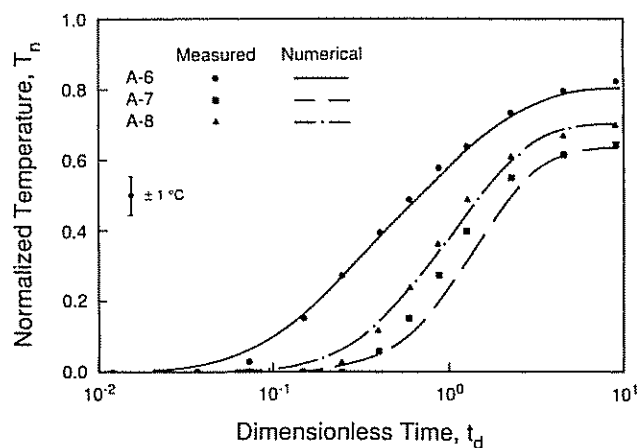


Fig. 8. Measured and predicted thermal responses for test 1.

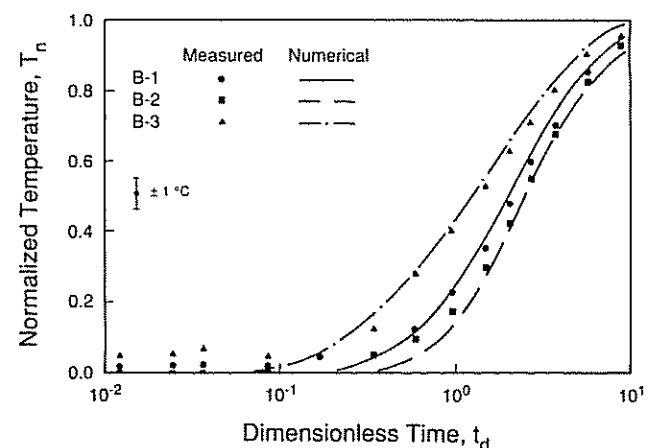


Fig. 10. Measured and predicted thermal responses for test 3.

The numerical model provides a method of simulating the response of the physical model under various test conditions. The incorporation of semiconfined behavior into the formulation of the numerical model and the application of boundary conditions accurately reflecting those experienced by the physical model serve to improve the agreement of the measured and predicted responses relative to that obtained using a nonleaky model with static boundary conditions. The ability to interpret the magnitude of heat transfer from the matrix to the disc system from apparent steady state conditions is significant in that these parameters would otherwise be difficult to quantify.

The constitutive relationship embodied in semiconfined behavior represents a simplification of the physics of the thermal model. Explicitly representing the heat transfer within the insulation and between the matrix and model discs requires either the discretization of the matrix or the utilization of more elegant, and computationally intensive, dual-porosity models. Regardless of the inherent simplification of the leakage model, the formulation appears to adequately predict the response of the physical model under the conditions of the tests. The residual predictive errors are thought to be entirely related to the limitations of the experimental procedure and not to a constitutive failure of the numerical model.

A detailed geometric description of the model and the results of the tests conducted on the model are available to researchers wishing to evaluate alternative numerical algorithms. Interested parties should contact the authors directly.

#### NOTATION

$b$	fracture aperture or disc thickness.
$d, d_d$	disc diameter, dimensionless diameter.
$h, \dot{h}, \mathbf{h}, \dot{\mathbf{h}}$	hydraulic head in fracture, time derivative of head, vector of nodal heads, and vector of time derivatives of nodal heads.
$h_r, \mathbf{h}_r$	reference hydraulic head in rock matrix, vector of reference heads.
$\mathbf{q}$	vector of specified nodal discharges.
$q_l, \mathbf{q}_l$	leakage volume per unit time, vector of nodal discharges due to leakage.
$q_s, \mathbf{q}_s$	storage depletion per unit time, vector of nodal discharges due to storage depletion.
$\mathbf{q}_c$	vector of nodal discharges due to conduction.
$t, t_d, \Delta t$	time, dimensionless time, and time increment.
$v_l$	leakage velocity.
$v_s$	storage depletion velocity.
$A$	plan area of fracture.
$D$	diffusivity.
$k'$	leakage coefficient.
$K$	conductivity.
$\mathbf{K}$	conductance matrix.
$\mathbf{L}$	lumped leakage matrix.
$S_s$	specific storage.
$\mathbf{S}$	lumped storativity matrix.
$T, T_{bc}, T_n, T_0$	temperature, boundary condition temperature, normalized temperature, and initial temperature.
$\mathbf{W}$	nodal weighting matrix.
$\delta_{ij}$	Kronecker delta.

versity. The fabrication and instrumentation of the physical model was made possible by grant G1154142 from the Pennsylvania Mining and Mineral Resources Research Institute, U.S. Department of the Interior, Bureau of Mines. This support is gratefully acknowledged.

#### REFERENCES

- American Society of Metals, *Metals Handbook*, 9th ed., vol. 2, pp. 323-325, American Society for Metals, Metals Park, Ohio, 1979.
- Andersson, J., and B. Dverstorp, Conditional simulations of fluid flow in three-dimensional networks of discrete fractures, *Water Resour. Res.*, 23(10), 1876-1886, 1987.
- Atkinson, K. E., *An Introduction to Numerical Analysis*, pp. 168-171, John Wiley, New York, 1978.
- Eckert, E. R. G., and R. M. Drake, *Heat and Mass Transfer*, 2nd ed., p. 504, McGraw-Hill, New York, 1959.
- Elsworth, D., A hybrid boundary element-finite element analysis procedure for fluid flow simulation in fractured rock masses, *Int. J. Numer. Anal. Meth. Geomech.*, 10, 569-584, 1986a.
- Elsworth, D., A model to evaluate the transient hydraulic response of three-dimensional sparsely fractured rock masses, *Water Resour. Res.*, 22(13), 1809-1819, 1986b.
- Elsworth, D., and A. R. Piggott, Physical and numerical analogues to fractured media flow, in *Proceedings of the 6th International Congress on Rock Mechanics*, vol. 1, pp. 93-97, A. A. Baikema, Rotterdam, 1987.
- Hantush, M. S., and C. E. Jacob, Nonsteady radial flow in an infinite leaky aquifer, *Eos Trans. AGU*, 36(1), 95-100, 1955.
- Huang, C., and D. D. Evans, A three-dimensional computer model to simulate fluid flow and contaminant transport through a rock fracture system, *Rep. NUREG/CR-4042*, U.S. Nucl. Reg. Comm., Washington, D. C., 1985.
- Hudson, J. A., and P. R. LaPointe, Printed circuits for studying rock mass permeability, *Int. J. Rock Mech. Min. Sci. Geomech.*, 17(5), 297-301, 1980.
- Hull, L. C., J. D. Miller, and T. M. Clemo, Laboratory and simulation studies of solute transport in fracture networks, *Water Resour. Res.*, 23(8), 1505-1513, 1987.
- Javandel, I., and P. A. Witherspoon, Use of thermal model to investigate the theory of transient flow to a partially penetrating well, *Water Resour. Res.*, 3(2), 591-597, 1967.
- Kruseman, G. P., and N. A. DeRidder, *Analysis and Evaluation of Pumping Test Data*, International Institute for Land Reclamation and Improvement, Wageningen, The Netherlands, 1983.
- Long, J. C. S., P. Gilmour, and P. A. Witherspoon, A model for steady fluid flow in random three-dimensional networks of disc-shaped fractures, *Water Resour. Res.*, 21(8), 1105-1115, 1985.
- Moench, A. F., Double-porosity models for a fissured groundwater reservoir with fracture skin, *Water Resour. Res.*, 20(7), 831-846, 1984.
- Piggott, A. R., A numerical procedure for the analysis of steady state fluid flow in systems of finite discontinuities, 74 pp., M. Eng. thesis, Univ. of Toronto, Toronto, Ont., 1986.
- Piggott, A. R., and D. Elsworth, Physical and numerical studies of a fracture system model, research report, Coll. of Earth and Miner. Sci., Pa. State Univ., University Park, 1987.
- Sharp, J. D., Fluid flow through fissured media, Ph.D. thesis, Imperial Coll., London, 1970.
- Tsang, Y. W., The effect of tortuosity on fluid flow through a single fracture, *Water Resour. Res.*, 20(9), 1209-1215, 1984.
- Turner, W. C., and J. F. Malloy, *Thermal Insulation Handbook*, pp. 203-275, Robert E. Krieger and McGraw-Hill, Malabar, Fla. and New York, 1981.
- Wilson, C., An investigation of laminar flow in fractured porous rocks, Ph.D. thesis, Univ. of Calif., Berkeley, 1970.

D. Elsworth, Waterloo Centre for Groundwater Research, University of Waterloo, Waterloo, Ont., Canada N2L 3G1.

A. R. Piggott, Department of Mineral Engineering, 104 Mineral Sciences Building, Pennsylvania State University, University Park, PA 16802.

(Received March 22, 1988;  
revised September 12, 1988;  
accepted September 26, 1988.)

*Acknowledgments.* Funding for this project was provided by the Department of Mineral Engineering of The Pennsylvania State Uni-